

IMECE2018-88052

DIRECT INK WRITING OF GRAPHENE OXIDE REINFORCED PDMS MATRIX COMPOSITES FOR IMPROVED MECHANICAL PROPERTIES

Chao Liu

Kazuo Inamori School of Engineering,
New York State College of Ceramics,
Alfred University
Alfred, NY, United States

Li Jiang

College of Engineering,
Tuskegee University,
Tuskegee, AL, United States

Junjun Ding*

Kazuo Inamori School of Engineering,
New York State College of Ceramics,
Alfred University
Alfred, NY, United States

INTRODUCTION

Polydimethylsiloxane (PDMS) has been extensively used in various applications, such as medical devices, cell culture, and soft robots due to its unique properties, which includes its biocompatibility, high transparency, moldability, and mechanical flexibility [1-4]. Various manufacturing techniques have been developed to fabricate PDMS, including soft lithography, molding, dip coating, and spin coating [5-9]. While those techniques are often useful for fabricating microstructures in two-dimensions (2D), they are limited to yield three-dimensional (3D) complex structures.

Additive manufacturing (AM), often referred to as 3D printing, is a popular method for rapid prototyping compared with traditional material subtracting machining methods in recent years. AM technology shows advantages including free form design, low cost, capable for small production quantities, and various feeding materials [10-12]. Materials in various forms such as powder, filament, and viscous ink have been printed out by methods including material jetting, material extrusion, powder bed fusion, binder jetting, direct energy deposition, and photo-polymerization. Common AM technologies are multi-jet printing (MJP), fused deposition modeling (FDM), selective laser sintering (SLS), stereolithography apparatus (SLA), and direct ink writing (DIW) [13-15]. MJP, similar to inkjet printing, jet-drops liquid photopolymer to create each layer with ultraviolet light curing. However, a drawback is that only low viscosity ink materials are available for printing [16]. FDM is the most widely applied material extrusion process due to its small footprint, low cost, and reliability [17, 18]. Filaments are

KEYWORDS

Polydimethylsiloxane, Graphene oxide, Direct ink writing

ABSTRACT

Recently, PDMS has been widely used because of its outstanding properties, such as its biocompatibility, moldability, and Mechanical Flexibility. However, the low mechanical strength hinders its ability for further applications. The Addition of graphene oxide (GO) into Polydimethylsiloxane (PDMS) matrices as a reinforcement is a reasonably simple way to improve its mechanical properties. Direct ink writing (DIW) is an ideal method for printing viscous materials which provides useful advantages for fabrication, such as higher design freedom, as well as having no requirement for a castable mold, compared to conventional PDMS processing methods. Herein, we demonstrate the DIW 3D printing of GO reinforced PDMS matrix composites. PDMS SE 1700 and Sylgard 184 were mixed in 4:1 and 7:3 ratios as matrix materials with controlled rheological properties. GO, synthesized by modified Hummer's method, was loaded into PDMS at various weight ratios (0.5%, 1%, 2%, 3% and 4%) to fabricate GO/PDMS composites. The GO dispersed uniformly throughout the PDMS matrix with no visible aggregation during the mixing and printing processes. Tensile tests were performed using 3D printed dog-bone shape GO/PDMS bars to evaluate the enhancement of the GO reinforcement. The results showed that the Young's modulus of PDMS increased by 58.7% with 1% GO reinforcement.

* Corresponding author.

Email address: dingj@alfred.edu (J. Ding)

extruded through a nozzle with an elevated temperature to deposit materials layer by layer. While thermoplastics and their composites are suitable for low cost desktop FDM 3D printing by melting and depositing the thermoplastics at extrusion nozzle, thermosets cannot be printed by FDM. DIW, also known as robocasting, is another material extrusion technique in which a filament of a paste or high viscosity ink is extruded from a nozzle to deposit materials layer by layer. The ink retains its shape immediately after exiting the printing nozzle, exploiting the rheological property of shear thinning [19, 20]. While DIW is initially designed for printing ceramic green bodies, it is also well-suited for fabricating viscoelastic polymers at room temperature [16, 21].

To successfully print thermoset materials such as PDMS by DIW, there are several issues that must be addressed. The low viscosity PDMS prepolymer and curing agent mixture requires a large amount of time for gelation to occur. The PDMS ink tends to reflow under gravity, thus the print fidelity is lost. Hinton et. al demonstrated the DIW of hydrophobic PDMS prepolymer resins using a hydrophilic Carbopol support via freedom reversible embedding [22]. The hydrophilic Carbopol bath confined 3D PDMS ink in the support gel for an extended time to allow for the PDMS ink cure. PDMS was also printed within an oil-based granular gel with a relatively high resolution (80 μm) and mechanical properties (700% strain) [23]. Another approach is to tune the inks rheological properties by blending two types of PDMS prepolymers together, showing 3D printed PDMS exhibits better cell adhesion properties in comparison with PDMS surfaces made by traditional casting methods [21]. The hindered mechanical strength of PDMS limits even broader applications for building devices with higher mechanical strength [24]. One way to correct for this limitation is to produce PDMS composites by adding reinforcement, such as carbon nanomaterials [25, 26], metal oxides [27], and silica [28]. In general, Graphene oxide (GO) is a good reinforcement to improve mechanical properties of polymeric materials due to the particular structure of the layers with respect to the oxygen functional groups present [29, 30]. Recently, many studies have focused on strengthening the mechanical properties of various polymers through the addition of GO. Chen et al. used the FDM method as a means of fabricating GO/thermoplastic polyurethane (TPU)/poly(lactic acid) (PLA) nanocomposites for improved tensile and compression moduli for various polymers [31]. Xu et al. fabricated poly(vinyl alcohol)(PVA)/GO composite films via vacuum filtration to improve the strength of PVA [32]. Rama et al. used a solvent casting technique to synthesize Sulfonated poly(ether-ether-ketone) functionalized graphene oxide (SPG)/poly(vinylidene fluoride) (PVDF) composites to increase the maximum elongation and stress at failure for PVDF samples [33]. Although extensive work has shown how GO reinforces thermoplastic materials in these studies, little research has been done on the improvement of mechanical properties with GO reinforced viscoelastic thermoset polymers produced via additive manufacturing method.

In this work, we fabricated GO reinforced PDMS matrix composites using the DIW method to improve their mechanical

strength. Highly viscous PDMS SE 1700 and low viscous Sylgard 184 were mixed in 4:1 and 7:3 ratios as printable inks for PDMS. GO/PDMS composites, each containing different weight percentages of GO (0.5%, 1%, 2%, 3% and 4%), were fabricated using GO, which was synthesized via a modified Hummer's method, and through utilization of a homemade DIW 3D printer. Tensile tests showed the tensile Young's modulus of PDMS composites increased 58.7% after loading of 1 wt% GO powder, indicating effective mechanical properties improvement by GO reinforcement in PDMS matrix.

METHOD

Materials: Graphite (powder, $\geq 99.0\%$, Acros Organics), sulfuric acid (H_2SO_4 , technical grade, 66° Baumé, Fisher Scientific), potassium permanganate (KMnO_4 , powder, 99%, Alfa Aesar), hydrogen peroxide (H_2O_2 , technical grade, 34-37%, Fisher Scientific) and muriatic acid (HCl, 31.45%, Sunnyside Corporation) were used to synthesize graphene oxide. Polydimethylsiloxane (PDMS) SE 1700 (Dow Corning,) and PDMS Sylgard 184 (Dow Corning) were used to fabricate the matrix of the composites.

Graphene Oxide Synthesis: A modified Hummer's method was implemented to synthesize GO. 1 g graphite and 30 mL H_2SO_4 were added slowly into a 300 mL beaker, which was placed on a stirrer at 350 rpm. An ice bath was set up to guarantee the temperature of the solution not exceeding 5 °C. Then 4 g KMnO_4 was added into the beaker. 3 hours later, the beaker was moved on a hot plate to keep the temperature of solution at 35 °C for 12 hours. Subsequently 150 mL deionized water was added into the beaker dropwise with the temperature controlled in an ice bath. Later, 3 mL H_2O_2 was added and the solution became bright brown. The product was centrifuged at 4000 rpm for 30 min at room temperature. After removing the upper liquid, the sediments were washed with 5% HCl and deionized water in order and centrifuged repeatedly. The remaining sediments were placed into a -80 °C freezer for 12 hours and moved to a -20 °C freeze drier afterwards. After 3 days, the freeze-dried GO is grounded into a fine powder via ball milling.

Ink preparation: First, the PDMS SE 1700 base and Sylgard 184 base were mixed with their curing agents separately at a weight ratio of 10:1 and stirred for 10 min. A vacuum desiccator was used for degassing for 20 min to remove air bubbles. A mixture of PDMS SE 1700 and Sylgard 184 was then prepared at four different ratios (10:0, 4:1, 3:2 and 0:10). GO powder (0.5%, 1%, 2%, 3% and 4%) was added into the viscoelastic mixture slowly. After stirring for 20 min, the black slurry was put into a vacuum desiccator again for degassing for 30 min. A 10 mL syringe barrel was used to load the slurry for the following 3D printing.

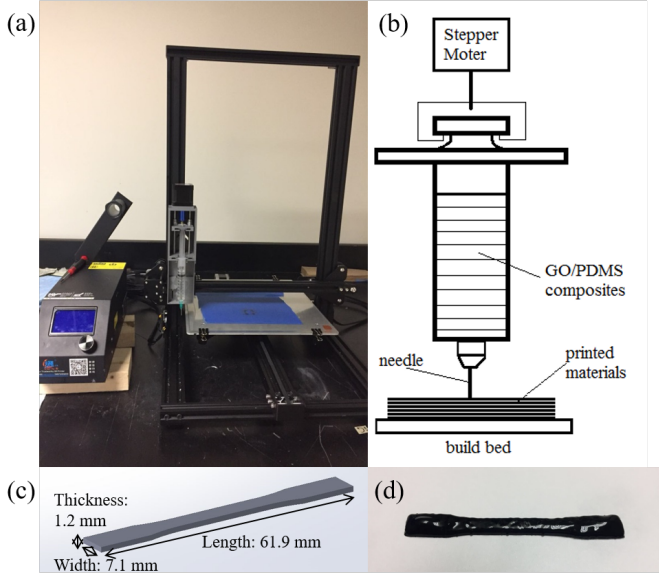


Figure 1. (a) Photo of our modified DIW 3D printer. (b) Schematic illustration of the syringe pump and its working process. (c) ASTM 638 tensile test model and its dimensions (d) Photo of a typical GO/PDMS composite tensile test part printed by DIW.

Direct ink writing: A homemade 3D printer was used for direct ink writing by modifying a desktop FDM 3D printer (Creality CR-10S), shown in Figure 1(a). The schematic working process with a syringe pump is shown in Figure 1(b). An 18 Ga (0.84 mm inner diameter) needle tip was used as the extruding nozzle. The printing speed was set as 3 mm/s and the layer height was set as 0.6 mm to compensate for the collapse of liquid materials.

Rheological test: TA Instruments AR2000 Rheometer was used to measure viscosity and shear stress of uncured ink. 40 mm parallel plate (Peltier plate steel-107296) was used as rotational element. All rheological tests were performed at 30 °C.

Characterization: Scanning electron microscope (SEM, Quanta 200F, FEI) was used to observe the dispersion of GO in PDMS matrix. Fourier transform infrared spectroscopy (FTIR Nicolet 6700, Thermo Fisher) and Raman spectroscopy (WITec alpha300) were used to characterize graphite and GO powder.

Mechanical test: Instron 5566 Universal Testing Machine was used to perform tensile tests. Dog-bone bars based on ASTM 638 were designed with 3D modeling software and printed at least five parts for each GO/PDMS composite samples to perform mechanical tensile testing. The dimensions of the dog-bone bars are shown in Figure 1(c). The as-printed component for tensile test is shown in Figure 1(d). The tensile rate was set to 5 mm/min.

RESULTS

Characterization

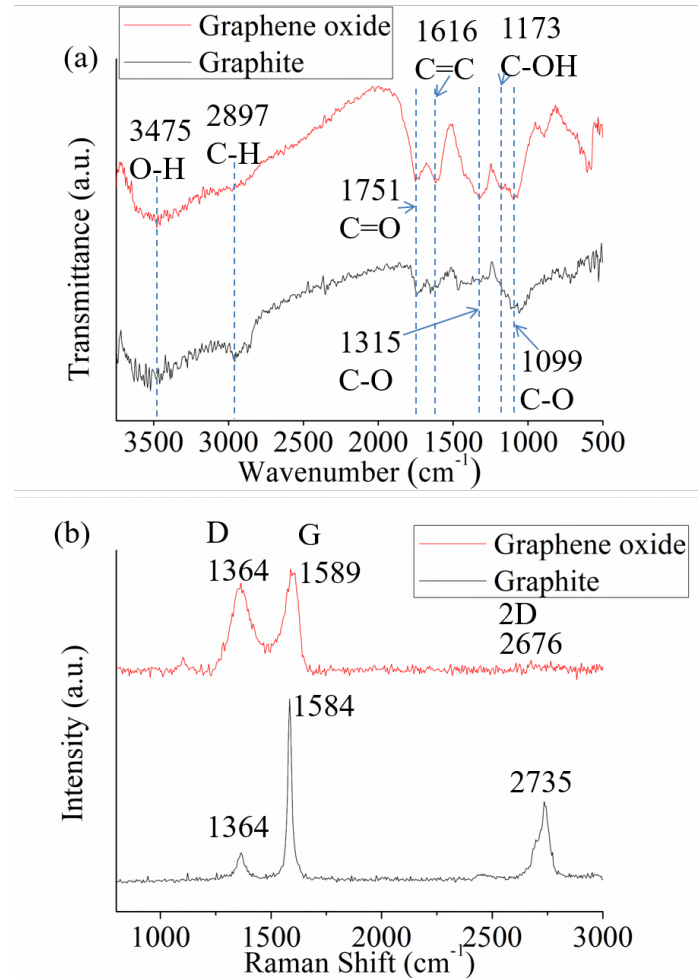


Figure 2. Characterizations of raw material graphite and synthesized GO. (a) Fourier transform infrared (FTIR) spectrum and (b) Raman spectrum.

To characterize the GO fabricated by using a modified version of Hummer's method, and to make a comparison with raw material graphite, FTIR and Raman spectroscopy analyses were performed. The results of transmittance FTIR spectroscopy are shown in Figure 2(a). The peaks at 1099 cm⁻¹, 1173 cm⁻¹, 1315 cm⁻¹, 1616 cm⁻¹, 1751 cm⁻¹, 2897 cm⁻¹ and 3475 cm⁻¹ represents C-O, C-OH, C-O, C=C, C=O, C-H and O-H, respectively [34, 35]. An abnormality was found from the graphite spectra collected, as there are oxygen functional groups existed in graphite, such as C=O at 1751 cm⁻¹ and C-O at 1099 cm⁻¹. The impurity of the powdered graphite is likely due to slight oxidation occurring while in storage. However, peaks of these two functional groups in graphite are significantly lower than those in GO, indicating more C=O and C-O at 1099 cm⁻¹ functional groups were created during the oxidation process. In addition, C-O at 1315 cm⁻¹ and C-OH at 1173 cm⁻¹ exist only in GO, also indicating the oxidation reaction. The Raman spectra of graphite and GO are shown in Figure 2(b). The higher intensity D-band, wider D-band, and G-band show the graphene layers become more disordered after the oxidation process [36].

Another significant difference between graphite and GO seen in the Raman spectra is that graphite shows distinct 2D-band at 2735 cm^{-1} , while GO show no 2D-band. The reason is that the synthesized functional groups inserted between graphene layers causes deformation of the graphitic chemical structure, which in turn, yields a change in the graphene layer's thickness [37].

Rheological test

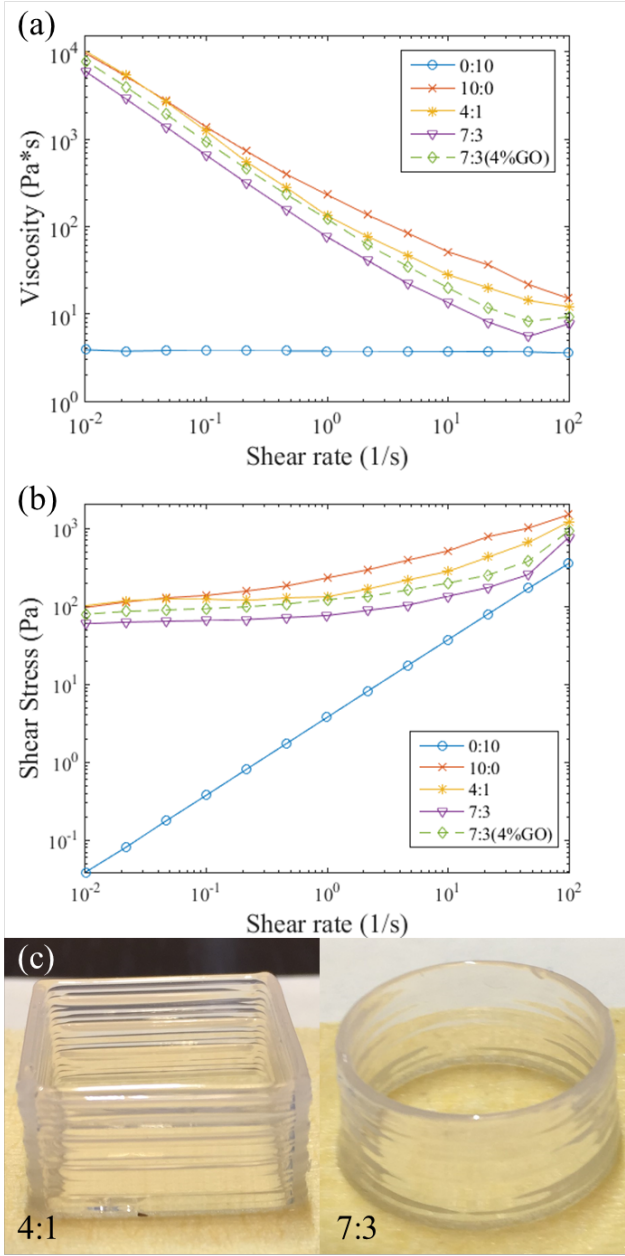


Figure 3. Rotational rheology test in various ratios of PDMS SE 1700 to Sylgard 184: (a) Viscosity vs shear rate from 0.01 s^{-1} to 100 s^{-1} . (b) Stress vs shear rate from 0.01 s^{-1} to 100 s^{-1} . The results of 4 wt% GO/PDMS composites are shown in dash line. (c) Basic shapes of 4:1 and 7:3 PDMS.

The rotational rheology test was performed to study the rheological properties of PDMS SE 1700, Sylgard 184 and the mixtures containing both of them. As shown in Figure 3(a), the viscosity of PDMS 0:10 (Sylgard 184 only) is $3.73 \pm 0.18\text{ Pa}\cdot\text{s}$, which remains constant and quite low with respect to increasing shear rate. In contrast, the viscosity of other samples decreases as the shear rate increases, which is the behavior of shear thinning [38]. In Figure 3(b), the shear stress of PDMS 0:10 increases with a constant linear slope as the shear rate increases. However, the shear stress of other samples increases non-linearly as shear rate increases. Both of viscosity and shear stress curves show that the Sylgard 184 behaves as a Newtonian fluid while other ratios of PDMS mixtures behave as non-Newtonian fluids. The long-chain molecules of non-Newtonian fluid (SE 1700) twine with each other at low flow rates, which makes the solution more viscous and easier to stack layer by layer. Pure Sylgard 184 could not hold up the shape without any support due to its low viscosity. While pure SE 1700 should be able to stack theoretically, the high viscosity prevents it from extruding through the small nozzle. Basic shapes could be printed using 4:1 and 7:3 mixing ratio PDMS ink, shown in Figure 3(c). Clearer boundaries between layers are observed in models printed by 4:1 PDMS ink, showing the combination of different layers. Apparently, the viscosity and shear stress increase gradually with the increasing ratio of SE 1700 to Sylgard 184 in Figure 3(a, b). To ensure that the GO/PDMS composites can be extruded from the nozzle and hold up their shape, 4 wt% GO mixed with a 7:3 PDMS matrix was also subject to rheological testing. The viscosity and shear stress of this sample in Figure 3(a, b) are located between the 4:1 and 7:3 PDMS samples, showing the theoretical printability of 4% GO/PDMS composites. Since the viscosity of these composites shows a positive correlation to the reinforcement content, the rheological properties of 0.5–3 wt% GO/PDMS composites should locate between curves of 7:3 PDMS matrix and 4 wt% GO/PDMS composites, indicating that the 0.5–3 wt% GO/PDMS composites are expected to be able to print.

Dispersion

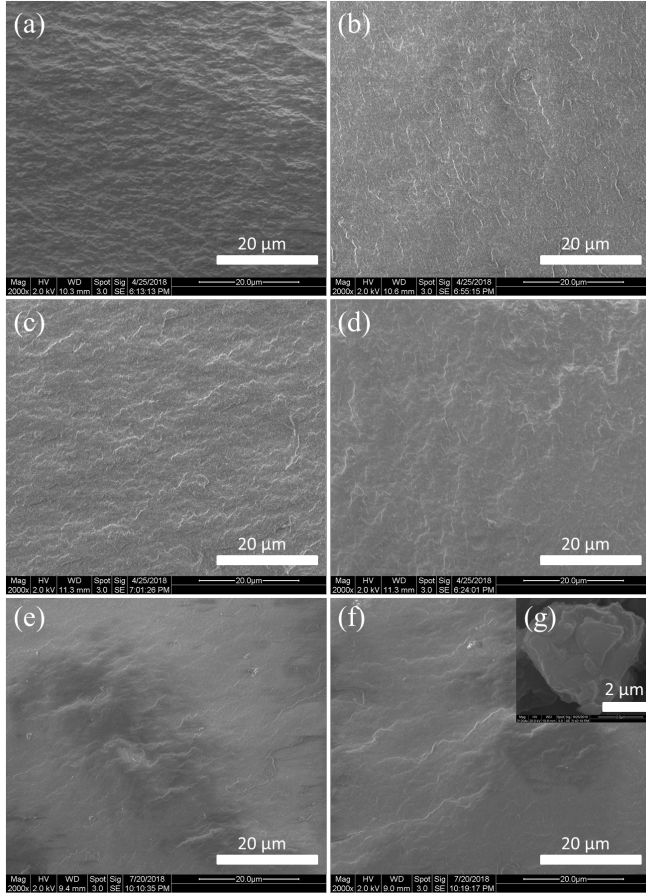


Figure 4. SEM images of fracture surface of different GO infill: (a) 0 wt% GO, (b) 0.5 wt% GO, (c) 1 wt% GO, (d) 2 wt% GO, (e) 3 wt% GO and (f) 4 wt% GO. (g) Single particle of graphene oxide.

SEM images of the torn cross-sections of varying GO concentrations in PDMS matrices are shown in Figure 4 to examine the dispersion of GO. Since the diameter of GO is around 5 μm , which is shown in Figure 4(g), no clear agglomeration of GO flakes were found to have occurred in the PDMS matrix in Figure 4(a-f), indicating that GO disperses uniformly within the PDMS matrix in the printed composites. In Figure 4(b-f), the flake geometries on the fracture surface indicates the existence of GO in comparison with the zero-GO infilled composite shown in Figure 4(a), which exhibited no such shapes. GO can be embedded and held in PDMS due to the rough microstructures of GO, and hydrogen bonding present within functional group branching off of the GO and PDMS [39, 40]. The increasing amount of infilled GO in PDMS leads to the increasing amount of flake shapes shown in Figure 4(b-f).

Mechanical test

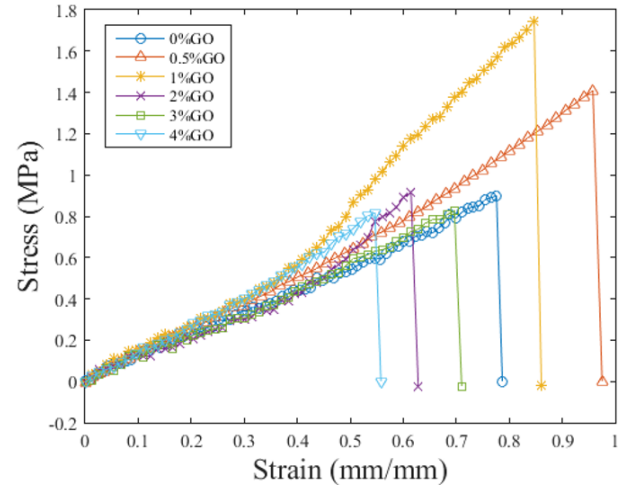
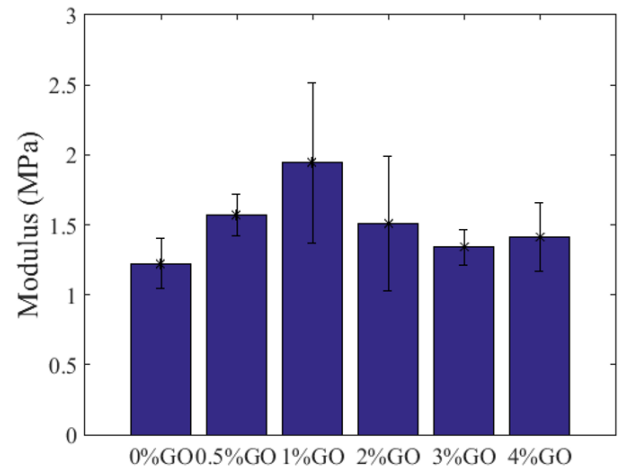


Figure 5. (a) Young's modulus of different GO infill (0%, 0.5%, 1%, 2%, 3% and 4%). (b) Tensile testing curves of different GO infill (0%, 0.5%, 1%, 2%, 3% and 4%).

Tensile tests were performed to investigate the mechanical properties of GO/PDMS composites. The tensile Young's modulus and stress-strain curves are shown in Figure 5(a) and 5(b), respectively. PDMS SE 1700 and Sylgard 184 were mixed in 7:3 ratio for all GO/PDMS composites. In Figure 5(a), the tensile modulus of PDMS increases from 1.224 MPa with no GO to 1.943 MPa with 1 wt% GO, indicating that the GO reinforcement improves the mechanical strength of PDMS by 58.7%. However, the modulus drops with further increased GO weight concentrations. With increasing GO content, the amount of microscale air bubbles formed was found to increase at the location of the fracture surface, affecting the cross-sectional area, resulting in inaccuracy of tensile stress and modulus data. Non-uniform mixing of GO and PDMS was also found to create defects within the composites, especially with respect to the increasing amount of reinforcement. In Figure 5(b), all tensile curves are all nearly linearly correlating, indicating that the tensile deformation of GO/PDMS composites is a result of elastic deformation. The 0.5 wt% GO shows the highest

maximum strain, while the maximum strain of higher concentration of GO in PDMS drops heavily as the concentration of GO increases. Although GO is a good reinforcement material for improving overall mechanical strength, the elasticity of the polymer decreases due to its rigid molecular structure.

CONCLUSIONS

In conclusion, this study demonstrates an effective AM method for fabricating PDMS and GO/PDMS composites by direct ink writing. Two different PDMS SE 1700 and Sylgard 184 were mixed in various ratios (10:0, 4:1, 7:3 and 0:10) to study the rheological properties for printable ink. SEM images of cross-sections from GO/PDMS composites show uniform dispersion of GO in PDMS formed, using GO fabricated from graphite by modified Hummer's method. Tensile tests show 58.7% tensile modulus improvement with 1 wt% GO in 7:3 PDMS matrix. The results show that GO reinforcement in the GO/PDMS composites effectively improves the mechanical strength.

ACKNOWLEDGMENTS

This work is supported by Faculty Startup Fund in New York State College of Ceramics at Alfred University. The authors would like to thank James Thiebaud, Guangran Zhang and Yiyu Li at Alfred University for the help of materials characterizations. The authors are also thankful to Ashley T Lenau and Benjamin R Zimmerli at Alfred University for assisting with editing and revisions of this paper.

REFERENCES

- [1] Jiang, Yusheng; Wang, Hui; Li, Shunbo and Wen, Weijia. "Applications of micro/nanoparticles in microfluidic sensors: a review." *Sensors* Vol. 14 No. 4 (2014): pp. 6952-6964.
- [2] Hua, Feng; Sun, Yugang; Gaur, Anshu; Meitl, Matthew A; Bilhaut, Lise; Rotkina, Lolita; Wang, Jingfeng; Geil, Phil; Shim, Moonsub and Rogers, John A. "Polymer imprint lithography with molecular-scale resolution." *Nano Letters* Vol. 4 No. 12 (2004): pp. 2467-2471.
- [3] Ding, Junjun; Fu, Shichen; Zhang, Runzhi; Boon, Eric; Lee, Woo; Fisher, Frank T and Yang, Eui-Hyeok. "Graphene—vertically aligned carbon nanotube hybrid on PDMS as stretchable electrodes." *Nanotechnology* Vol. 28 No. 46 (2017): pp. 465302.
- [4] Zhang, Runzhi; Ding, Junjun; Liu, Chao and Yang, Eui-Hyeok. "Highly stretchable supercapacitors enabled by interwoven CNTs partially embedded in PDMS." *ACS Applied Energy Materials* Vol. 1 No. 5 (2018): pp. 2048-2055.
- [5] Chang-Yen, David A; Eich, Richard K and Gale, Bruce K. "A monolithic PDMS waveguide system fabricated using soft-lithography techniques." *Journal of Lightwave Technology* Vol. 23 No. 6 (2005): pp. 2088-2093.
- [6] Shih, Teng-Kai; Chen, Chia-Fu; Ho, Jeng-Rong and Chuang, Fang-Tzu. "Fabrication of PDMS (polydimethylsiloxane) microlens and diffuser using replica molding." *Microelectronic Engineering* Vol. 83 No. 11-12 (2006): pp. 2499-2503.
- [7] Lee, Haeshin; Lee, Bruce P and Messersmith, Phillip B. "A reversible wet/dry adhesive inspired by mussels and geckos." *Nature* Vol. 448 No. 7151 (2007): pp. 338-341.
- [8] Mata, Alvaro; Fleischman, Aaron J and Roy, Shuvo. "Characterization of polydimethylsiloxane (PDMS) properties for biomedical micro/nanosystems." *Biomedical Microdevices* Vol. 7 No. 4 (2005): pp. 281-293.
- [9] Ding, Junjun; Fisher, Frank T. and Yang, Eui-Hyeok. "Direct transfer of corrugated graphene sheets as stretchable electrodes." *Journal of Vacuum Science & Technology B, Nanotechnology and Microelectronics: Materials, Processing, Measurement, and Phenomena* Vol. 34 No. 5 (2016): pp. 051205.
- [10] Mueller, Bernhard. "Additive manufacturing technologies—rapid prototyping to direct digital manufacturing." *Assembly Automation* Vol. 32 No. 2 (2012).
- [11] Conner, Brett P; Manogharan, Guha P; Martof, Ashley N; Rodomsky, Lauren M; Rodomsky, Caitlyn M; Jordan, Dakesha C and Limperos, James W. "Making sense of 3-D printing: creating a map of additive manufacturing products and services." *Additive Manufacturing* Vol. 1 No. (2014): pp. 64-76.
- [12] Panesar, Ajit; Ashcroft, Ian; Brackett, David; Wildman, Ricky and Hague, Richard. "Design framework for multifunctional additive manufacturing: coupled optimization strategy for structures with embedded functional systems." *Additive Manufacturing* Vol. 16 No. (2017): pp. 98-106.
- [13] Barclift, Michael W and Williams, Christopher B. "Examining variability in the mechanical properties of parts manufactured via polyjet direct 3D printing," *International Solid Freeform Fabrication Symposium*. pp. 876-890. Austin, Texas, August 6-8, 2012.
- [14] Bikas, H; Stavropoulos, Panagiotis and Chryssolouris, George. "Additive manufacturing methods and modelling approaches: a critical review." *The International Journal of Advanced Manufacturing Technology* Vol. 83 No. 1-4 (2016): pp. 389-405.
- [15] Zhou, Nanjia; Liu, Chengye; Lewis, Jennifer A and Ham, Donhee. "Gigahertz electromagnetic structures via direct ink writing for radio - frequency oscillator and transmitter applications." *Advanced Materials* Vol. 29 No. 15 (2017): pp. 1605198.
- [16] Chen, Bolin; Jiang, Yizhou; Tang, Xiaohui; Pan, Yayue and Hu, Shan. "Fully packaged carbon nanotube supercapacitors by direct ink writing on flexible substrates." *ACS Applied Materials & Interfaces* Vol. 9 No. 34 (2017): pp. 28433-28440.
- [17] Ning, Fuda; Cong, Weilong; Qiu, Jingjing; Wei, Junhua and Wang, Shiren. "Additive manufacturing of carbon fiber reinforced thermoplastic composites using fused deposition modeling." *Composites Part B: Engineering* Vol. 80 No. (2015): pp. 369-378.
- [18] Mohamed, Omar Ahmed; Masood, Syed Hasan and Bhowmik, Jahar Lal. "Experimental investigation of time-dependent mechanical properties of PC-ABS prototypes processed by FDM additive manufacturing process." *Materials Letters* Vol. 193 No. (2017): pp. 58-62.
- [19] Rueschhoff, Lisa; Costakis, William; Michie, Matthew; Youngblood, Jeffrey and Trice, Rodney. "Additive

- manufacturing of dense ceramic parts via direct ink writing of aqueous alumina suspensions." *International Journal of Applied Ceramic Technology* Vol. 13 No. 5 (2016): pp. 821-830.
- [20] Lewis, Jennifer A; Smay, James E; Stuecker, John and Cesarano, Joseph. "Direct ink writing of three - dimensional ceramic structures." *Journal of the American Ceramic Society* Vol. 89 No. 12 (2006): pp. 3599-3609.
- [21] Ozbolat, Veli; Dey, Madhuri; Ayan, Bugra; Povilanskas, Adomas; Demirel, Melik C and Ozbolat, Ibrahim T. "3D printing of PDMS improves its mechanical and cell adhesion properties." *ACS Biomaterials Science & Engineering* Vol. 4 No. 2 (2018): pp. 682-693.
- [22] Hinton, Thomas J; Hudson, Andrew; Pusch, Kira; Lee, Andrew and Feinberg, Adam W. "3D printing PDMS elastomer in a hydrophilic support bath via freeform reversible embedding." *ACS Biomaterials Science & Engineering* Vol. 2 No. 10 (2016): pp. 1781-1786.
- [23] O'Bryan, Christopher S; Bhattacharjee, Tapomoy; Hart, Samuel; Kabb, Christopher P; Schulze, Kyle D; Chilakala, Indrasena; Sumerlin, Brent S; Sawyer, W Gregory and Angelini, Thomas E. "Self-assembled micro-organogels for 3D printing silicone structures." *Science Advances* Vol. 3 No. 5 (2017): pp. e1602800.
- [24] Mi, Hao-Yang; Jing, Xin; Huang, Han-Xiong and Turng, Lih-Sheng. "Novel polydimethylsiloxane (PDMS) composites reinforced with three-dimensional continuous silica fibers." *Materials Letters* Vol. 210 No. (2018): pp. 173-176.
- [25] Chen, Zongping; Ren, Wencai; Gao, Libo; Liu, Bilu; Pei, Songfeng and Cheng, Hui-Ming. "Three-dimensional flexible and conductive interconnected graphene networks grown by chemical vapour deposition." *Nature Materials* Vol. 10 No. 6 (2011): pp. 424-428.
- [26] Compton, Brett G and Lewis, Jennifer A. "3D - printing of lightweight cellular composites." *Advanced Materials* Vol. 26 No. 34 (2014): pp. 5930-5935.
- [27] Maiga, Abdoul Kader, "Swelling-etching characterization of copper (I) oxide–PDMS for the development of micro/nano-particles composite MEMS corrosion sensor," Master Thesis. University of Arkansas, Fayetteville, AR. 2015.
- [28] Camenzind, Adrian; Schweizer, Thomas; Sztucki, Michael and Pratsinis, Sotiris E. "Structure & strength of silica-PDMS nanocomposites." *Polymer* Vol. 51 No. 8 (2010): pp. 1796-1804.
- [29] Dreyer, Daniel R.; Park, Sungjin; Bielawski, Christopher W. and Ruoff, Rodney S. "The chemistry of graphene oxide." *Chemical Society Reviews* Vol. 39 No. 1 (2010): pp. 228-240.
- [30] Gupta, Bhavana; Kumar, Niranjan; Panda, Kalpataru; Kanan, Vigneshwaran; Joshi, Shailesh and Visoly-Fisher, Iris. "Role of oxygen functional groups in reduced graphene oxide for lubrication." *Scientific Reports* Vol. 7 No. (2017): pp. 45030.
- [31] Chen, Qiyi; Mangadlao, Joey Dacula; Wallat, Jaqueline; De Leon, Al; Pokorski, Jonathan K and Advincula, Rigoberto C. "3D printing biocompatible polyurethane/poly (lactic acid)/graphene oxide nanocomposites: anisotropic properties." *ACS Applied Materials & Interfaces* Vol. 9 No. 4 (2017): pp. 4015-4023.
- [32] Xu, Yuxi; Hong, Wenjing; Bai, Hua; Li, Chun and Shi, Gaoquan. "Strong and ductile poly (vinyl alcohol)/graphene oxide composite films with a layered structure." *Carbon* Vol. 47 No. 15 (2009): pp. 3538-3543.
- [33] Layek, Rama K; Das, Ashok Kumar; Park, Min Jun; Kim, Nam Hoon and Lee, Joong Hee. "Enhancement of physical, mechanical, and gas barrier properties in noncovalently functionalized graphene oxide/poly (vinylidene fluoride) composites." *Carbon* Vol. 81 No. (2015): pp. 329-338.
- [34] Kumar, N; Das, S; Bernhard, C and Varma, GD. "Effect of graphene oxide doping on superconducting properties of bulk MgB₂." *Superconductor Science and Technology* Vol. 26 No. 9 (2013): pp. 095008.
- [35] Zhong, Linlin and Yun, Kyusik. "Graphene oxide-modified ZnO particles: synthesis, characterization, and antibacterial properties." *International Journal of Nanomedicine* Vol. 10 No. Special Issue (2015): pp. 79-92.
- [36] Kim, Hyo Jin; Lee, Sung-Min; Oh, Yoon-Suk; Yang, Young-Hwan; Lim, Young Soo; Yoon, Dae Ho; Lee, Changgu; Kim, Jong-Young and Ruoff, Rodney S. "Unoxidized graphene/alumina nanocomposite: fracture-and wear-resistance effects of graphene on alumina matrix." *Scientific Reports* Vol. 4 No. (2014): pp. 5176.
- [37] Kaniyoor, Adarsh and Ramaprabhu, Sundara. "A Raman spectroscopic investigation of graphite oxide derived graphene." *AIP Advances* Vol. 2 No. 3 (2012): pp. 032183.
- [38] Partal, Pedro and Franco, José M^a. "Non-newtonian fluids." *Rheology: encyclopaedia of life support systems (EOLSS)*. EOLSS Publications, Oxford (2010): pp. 96-119.
- [39] Huang, Hua-Dong; Ren, Peng-Gang; Xu, Jia-Zhuang; Xu, Ling; Zhong, Gan-Ji; Hsiao, Benjamin S and Li, Zhong-Ming. "Improved barrier properties of poly (lactic acid) with randomly dispersed graphene oxide nanosheets." *Journal of Membrane Science* Vol. 464 No. (2014): pp. 110-118.
- [40] Rafiee, Mohammad A; Rafiee, Javad; Wang, Zhou; Song, Huaihe; Yu, Zhong-Zhen and Koratkar, Nikhil. "Enhanced mechanical properties of nanocomposites at low graphene content." *ACS Nano* Vol. 3 No. 12 (2009): pp. 3884-3890.